JACS
JOURNAL OF THE AMERICAN CHEMICAL SOCIETY
Communication
pubs.acs.org/JACS

Surface Plasmon Resonance in Gold Ultrathin Nanorods and Nanowires

Ryo Takahata,[†] Seiji Yamazoe,[†,‡] Kiichirou Koyasu,[†,‡] and Tatsuya Tsukuda*[,†,‡]

[†]Department of Chemistry, School of Science, The University of Tokyo, 7-3-1 Hongo, Bunkyo-ku, Tokyo 113-0033, Japan
[‡]Elements Strategy Initiative for Catalysts and Batteries (ESICB), Kyoto University, Katsura, Kyoto 615-8520, Japan

Supporting Information

ABSTRACT: We synthesized and measured optical extinction spectra of Au ultrathin (diameter: ∼1.6 nm) nanowires (UNWs) and nanorods (UNRs) with controlled lengths in the range 20−400 nm. The Au UNWs and UNRs exhibited a broad band in the IR region whose peak position was red-shifted with the length. Polarized extinction spectroscopy for the aligned Au UNWs indicated that the IR band is assigned to the longitudinal mode of the surface plasmon resonance.

Following the publication of various reports on chemical synthesis between 2007 and 2009,[1−5] ultrathin gold nanowires (UNWs) with a diameter of <2 nm and a length on the μm scale have attracted much attention due to their unique structural, optical, electrical, and mechanical properties. Thanks to their novel properties, Au UNWs show promise for a variety of applications,[6−14] including mechanical energy storage devices,[6] pressure sensors with fast response, high sensitivity and good stability,[7] flexible electrodes with high transparency and metallic conductivity,[8] biosensors using an electrochemical and near-infrared photoacoustic imaging method,[9,10] surface-enhanced Raman scattering,[5] and catalysis.[11]

Regardless of growing interest in the application of Au UNWs, their fundamental properties such as stability and optical properties are less well understood than those of conventional gold nanostructures such as nanospheres (NSs) and nanorods (NRs). Classical molecular dynamics simulation suggests that the surfactant not only acts as a soft template for controlling the morphology of the Au UNWs[2,3] but also enhances the thermal stability of the UNWs.[15] As for the optical properties, Au UNWs are expected to exhibit a single extinction band associated with the longitudinal surface plasmon resonance (SPR) mode on the basis of the well-established optical properties of Au NSs and NRs.[16−18] Recent time-dependent density functional theory calculations[19−22] indicated the presence of the longitudinal SPR mode and the red shift with the length. However, experimental data on the optical properties of Au UNWs are limited in the UV−visible region.[4,9] In this work, we present for the first time the whole profile of the optical spectrum of a highly purified sample of Au UNWs. The spectrum exhibited a broad and intense band in the IR region without an SPR band at ∼520 nm. This IR band was assigned to the longitudinal mode of SPR based on the dependence of the peak position on the length and the dependence of the extinction on the angle between the electronic vector of incident light and the long axis of the UNWs.

Highly purified Au UNWs were obtained by removing the Au NSs from crude UNWs prepared by the reported method.[5] Gold ultrathin nanorods (UNRs), defined in this paper as materials that have a diameter of less than 2 nm and an aspect ratio of 5−50, were successfully synthesized by a slightly modified method of synthesizing Au UNWs.[5] Details of the synthesis are given in the Supporting Information (SI). In brief, oleylamine and $HAuCl_4{\cdot}4H_2O$ were mixed in cyclohexane and stirred for 2 h (solution **a**). The color of solution **a** changed from orange to yellow upon addition of oleylamine due to the reduction of Au(III) to Au(I) (Figure S1). Solution **a** was diluted 8 and 16 times with cyclohexane to obtain solutions **b** and **c**, respectively. Then, triisopropylsilane was added to solutions **a**−**c**. Upon addition, the color changed gradually from yellow to brown within 6−30 h (Figure S1). Finally, Au UNWs and UNRs were precipitated by lowering the solution temperature and collected by filtration. Optical spectroscopy (Figure S2) and TEM analysis (Figure S3) of the filtrates indicated that the Au NSs (average diameter: ∼2.5 nm) contained were successfully removed in this step. The precipitates obtained from solutions **a**, **b**, and **c** are hereafter referred to as samples **A**, **B**, and **C**, respectively.

Figure 1 shows TEM images of samples **A**−**C** represented on the same scale. Sample **A** is not contaminated with NSs, but is dominated by UNWs with a diameter of ∼1.7 nm (Figures 1a, S4). The average length of Au UNWs in sample **A** is ∼400 nm although the distribution is rather broad (Figure 1b). The Au UNWs in sample **A** tend to form bundles due to van der Waals forces between oleylamine layers (Figure S5), as reported previously.[1,2,5] TEM images of samples **B** and **C** (Figures 1c, 1e) showed Au UNRs with a common diameter of ∼1.6 nm (Figure S4), but with significantly different lengths of ∼40 and ∼20 nm, respectively (Figures 1d, 1f). These Au UNWs and UNRs did not degrade after storage in the powder form at −20 °C for 3 months (Figure S6). The method of synthesizing Au UNRs developed here is easier than the reported method using amorphous Fe NSs as a reductant.[23] It was proposed that the one-dimensional assembly of Au(I) formed via aurophilic interaction acts as a precursor of the UNWs.[2,3] Successful synthesis of Au UNRs in the present study is ascribed to the reduction of the average length of the Au(I) assemblies by the dilution.

Received: April 10, 2014
Published: June 5, 2014

dx.doi.org/10.1021/ja503558c | J. Am. Chem. Soc. 2014, 136, 8489−8491

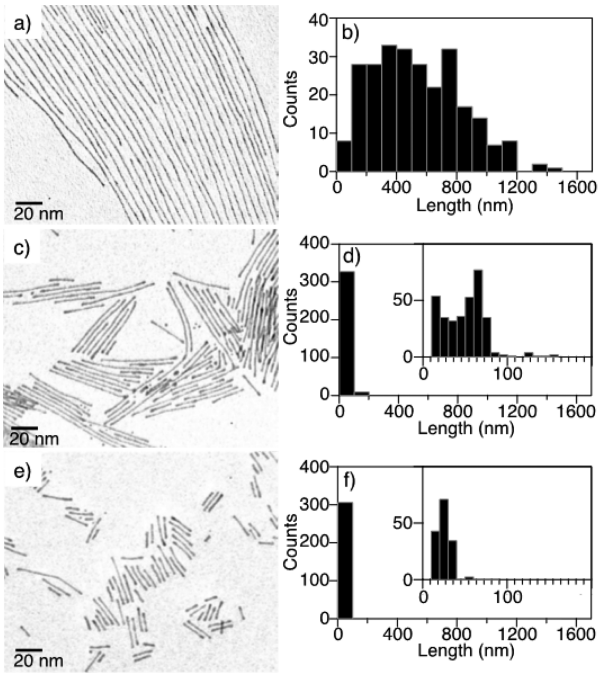

Figure 1. Typical TEM images and length distributions of samples **A** (a, b), **B** (c, d), and **C** (e, f). The insets of panels d and f show the histograms with smaller steps.

Optical extinction spectra of samples **A**–**C** are shown in Figure 2. Red curves represent UV–vis–near-IR (300–1600 nm) spectra recorded in cyclohexane dispersion. Blue and green curves show the mid-IR (1500–25 000 nm) spectra of samples cast on a KBr plate and the far-IR (15 000–100 000 nm) spectrum of sample **A** cast on a polyethylene film, respectively. Note that the sharp peaks in the IR spectra indicated by asterisks are assigned to vibrational peaks of oleylamine. The UV–vis spectra of samples **A**–**C** exhibit peaks at ~490 nm as indicated by the downward arrows. These peaks are not assigned to the SPR of Au NSs since the samples did not contain the Au NSs, but imply quantized electronic structures. In sample **A**, the extinction starts to increase with the wavelength from ~1000 nm (Figure 2a) as reported previously.[9] A broad band centered at ~20 μm was observed for the first time in sample **A** (Figure 2a). According to theoretical predictions,[19−22] it is plausible to assign this band to the longitudinal mode of SPR of Au UNWs. Comparison with the optical spectra of Au UNRs with shorter lengths lends further support to this assignment. The peak position is blue-shifted to ~6.0 μm for sample **B** (Figure 2b) and further to ~2.3 μm for sample **C** (Figure 2c). This length-dependent behavior is similar to that observed in the Au NRs[14] and is consistent with the theoretical predictions for ultrasmall gold NRs[19−22] and linear chains of Au_{13} superatoms.[24] It is difficult, however, to quantitatively correlate the observed SPR wavelength to the length because of the following reasons: (1) there is a measurable width in the length distribution (Figure 1); (2) the SPR wavelength may be shifted by plasmonic coupling between the bundled UNWs and UNRs as observed in Au NRs;[25−27] (3) chemical modification by oleylamine may induce the red shift of the SPR band of the UNWs and UNRs by reducing the electron conductivity as observed in small Ag NSs.[28]

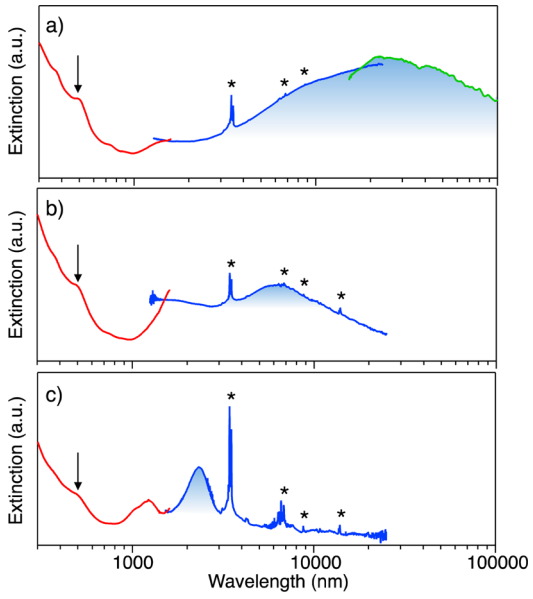

Figure 2. Optical spectra of (a) samples **A**, (b) **B**, and (c) **C** in UV–vis–near-IR (red), mid-IR (blue), and far-IR regions (green). The peaks indicated by asterisks were due to oleylamine.

In order to establish that the IR band corresponds to the longitudinal mode of SPR of Au UNWs, we measured polarized extinction spectra of the UNWs aligned in one direction on a glass plate. To immobilize the UNWs while controlling the alignment, a glass plate was immersed in a cyclohexane dispersion of sample **A** and cyclohexane was slowly evaporated (see Supporting Information and Figure S7). The morphology of the UNWs thus immobilized was examined by atomic force microscopy (AFM). Figure 3a shows a typical AFM image of the UNWs on a glass plate: the air/liquid interface is perpendicular to the *y*-axis in Figure 3a. Most of the UNWs were aligned perpendicular to the air/liquid interface probably due to the surface tension exerted perpendicularly to the interface. The preferential alignment of the UNWs along the *y*-axis was reproduced qualitatively although the degree of alignment was dependent on the batch mainly due to poor reproducibility of the evaporation rate. Figure 3b shows the height profile along the white line shown in Figure 3a. The average height of the peaks was ~4 nm corresponding to the summation of the diameter of the UNWs and the width of the oleylamine layer. In Figure 3a, thicker structures were also observed. The high-resolution AFM image (Figure 3c)

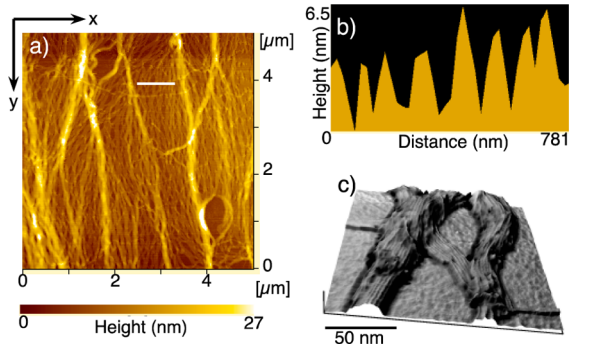

Figure 3. (a) AFM image, (b) height profile along the white line, and (c) high-resolution image of the Au UNWs immobilized on the glass plate. The *x*-axis in panel (a) is parallel to the air/liquid interface.

dx.doi.org/10.1021/ja503558c | J. Am. Chem. Soc. 2014, 136, 8489–8491

indicates that the thicker structures are bundles of individual UNWs.

We measured the polarized extinction spectra of the Au UNWs thus aligned as a function of the angle (θ) between the electric field of the polarized light and the y-axis (Figure 3a). Typical extinction spectra recorded at polarization angles of θ = 0° (blue) and 90° (red) are shown in Figure 4a. The extinction

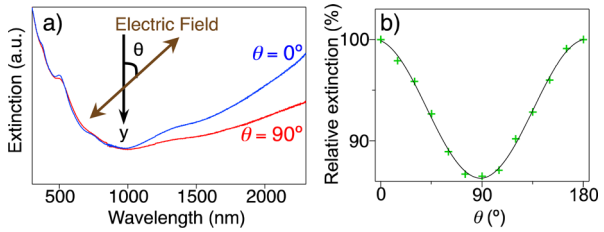

Figure 4. (a) The polarized extinction spectra recorded at θ = 0° (blue line) and 90° (red line). (b) Angle dependence of relative extinction at 2300 nm.

in the IR region is enhanced at θ = 0° where the incident light is polarized parallel to the long axis of the UNWs compared with that observed at θ = 90° where the incident light is polarized perpendicular to the long axis of the UNWs. Figure 4b plots the relative extinction at 2300 nm as a function of θ. Incomplete suppression of the IR extinction at θ = 90° (Figure 4) is due to imperfect alignment of the Au UNWs (Figure 3a). This angular dependence of the extinction spectra supports that the IR band is assigned to the longitudinal mode of SPR. A similar discussion has been made on Au NRs aligned in a poly(vinyl alcohol) film and along multiwall carbon nanotubes.[29,30]

In summary, we developed a method of synthesizing highly pure Au UNWs and UNRs with a common diameter of ∼1.6 nm but with different lengths. These one-dimensional structures exhibit strong extinction bands in the IR region. These bands are assigned to longitudinal modes of surface plasmon resonance on the basis of the length-dependent peak shift and polarization-angle dependent extinction change.

■ ASSOCIATED CONTENT

Supporting Information

Details of synthesis and characterization, measurements, and analysis. This material is available free of charge via the Internet at http://pubs.acs.org.

■ AUTHOR INFORMATION

Corresponding Author

tsukuda@chem.s.u-tokyo.ac.jp.

Notes

The authors declare no competing financial interest.

■ ACKNOWLEDGMENTS

We thank Prof. T. Teranishi and Dr. M. Sakamoto (Kyoto University) for valuable discussions. This research was financially supported by the Funding Program for Next Generation World-Leading Researchers (NEXT Program) (GR-003). We thank JASCO and Shimadzu for the measurement of far-IR spectra and high-resolution AFM images, respectively.

■ REFERENCES

(1) Halder, A.; Ravishankar, N. *Adv. Mater.* **2007**, *19*, 1854.
(2) Lu, X.; Yavuz, S.; Tuan, H.-Y.; Korgel, B. A.; Xia, Y. *J. Am. Chem. Soc.* **2008**, *130*, 8900.
(3) Hou, Z.; Tsung, X.-K.; Huang, W.; Zhang, X.; Yang, P. *Nano Lett.* **2008**, *8*, 2041.
(4) Pazos-Perez, N.; Baranov, D.; Irsen, S.; Hilgendorff, M.; Liz-Marzán, L. M.; Giersig, M. *Langmuir* **2008**, *24*, 9855.
(5) Feng, H.; Yang, Y.; You, Y.; Li, G.; Guo, J.; Yu, T.; Shen, Z.; Wu, T.; Xing, B. *Chem. Commun.* **2009**, 1984.
(6) Xu, J.; Wang, H.; Liu, C.; Yang, Y.; Chen, T.; Wang, Y.; Wang, F.; Liu, X.; Xing, B.; Chen, H. *J. Am. Chem. Soc.* **2010**, *132*, 11920.
(7) Gong, S.; Schwalb, W.; Wang, Y.; Chen, Y.; Tang, Y.; Si, J.; Shirinzadeh, B.; Cheng, W. *Nat. Commun.* **2014**, *5*, 3132.
(8) Azulai, D.; Belenkova, T.; Gilon, H.; Barkay, Z.; Markovich, G. *Nano Lett.* **2009**, *9*, 4246.
(9) Cui, H.; Hong, C.; Ying, A.; Yang, X.; Ren, S. *ACS Nano* **2013**, *7*, 7805.
(10) Koposova, E.; Kisner, A.; Shumilova, G.; Ermolenko, Y.; Offenhäusser, A.; Mourzina, Y. *J. Phys. Chem. C* **2013**, *117*, 13944.
(11) Hu, L.; Cao, X.; Yang, J.; Li, M.; Hong, H.; Xu, Q.; Ge, J.; Wang, L.; Lu, J.; Chen, L.; Gu, H. *Chem. Commun.* **2011**, *47*, 1303.
(12) Pud, S.; Kisner, A.; Heggen, M.; Belaineh, D.; Temirov, R.; Simon, U.; Offenhäusser, A.; Mourzina, Y.; Vitusevich, S. *Small* **2013**, *9*, 846.
(13) Chandri, U.; Kundu, P.; Singh, A. K.; Ravishankar, N.; Ghosh, A. *ACS Nano* **2011**, *5*, 8398.
(14) Chandri, U.; Kundu, P.; Kundu, S.; Ravishankar, N.; Ghosh, A. *Adv. Mater.* **2013**, *25*, 2486.
(15) Huber, S. E.; Warakulwit, C.; Limtrakul, J.; Tsukuda, T.; Probst, M. *Nanoscale* **2012**, *4*, 585.
(16) Kelly, K. L.; Coronado, E.; Zhao, L. L.; Schatz, G. C. *J. Phys. Chem. B* **2003**, *107*, 668.
(17) Murphy, C. J.; Sau, T. K.; Gole, A. M.; Orendorff, C. J.; Gao, J.; Gou, L.; Hunyadi, S. E.; Li, T. *J. Phys. Chem. B* **2005**, *109*, 13857.
(18) Pérez-Juste, J.; Pastoriza-Santos, I.; Liz-Marzán, L. M.; Mulvaney, P. *Coord. Chem. Rev.* **2005**, *249*, 1870.
(19) Guîdez, E. B.; Aikens, C. M. *J. Phys. Chem. C* **2013**, *117*, 12325.
(20) Piccini, G. M.; Havenith, R. W. A.; Broer, R.; Stener, M. *J. Phys. Chem. C* **2013**, *117*, 17196.
(21) Burgess, R. W.; Keast, V. J. *J. Phys. Chem. C* **2014**, *118*, 3194.
(22) López-Lozano, X.; Barron, H.; Mottet, C.; Weissker, H.-C. *Phys. Chem. Chem. Phys.* **2014**, *16*, 1820.
(23) Li, Z.; Tao, J.; Lu, X.; Zhu, Y.; Xia, Y. *Nano Lett.* **2008**, *8*, 3052.
(24) Maola, S.; Lehtovaara, L.; Häkkinen, H. *J. Phys. Chem. Lett.* **2014**, *5*, 1329.
(25) Jain, P. K.; Eustis, S.; El-Sayed, M. A. *J. Phys. Chem. B* **2006**, *110*, 18243.
(26) Jain, P. K.; Huang, W.; El-Sayed, M. A. *Nano Lett.* **2007**, *7*, 2080.
(27) Ghosh, S. K.; Pal, T. *Chem. Rev.* **2007**, *107*, 4797.
(28) Peng, S.; McMahon, J. M.; Schatz, G. C.; Gray, S. K.; Sun, Y. *Proc. Natl. Acad. Sci. U.S.A.* **2010**, *107*, 14530.
(29) van der Zande, B. M. I.; Pagès, L.; Hikmet, R. A. M.; van Blaaderen, A. *J. Phys. Chem. B* **1999**, *103*, 5761.
(30) Correa-Duarte, M. A.; Pérez-Juste, J.; Sánchez-Iglesias, A.; Giersig, M.; Liz-Marzán, L. M. *Angew. Chem., Int. Ed.* **2005**, *44*, 4375.